

Heat capacity studies on single crystal annealed Fe₃O₄

John P. Shepherd*

Department of Physics, Purdue University, West Lafayette, Indiana 47907

J. W. Koenitzer and Ricardo Aragón

Department of Chemistry, Purdue University, West Lafayette, Indiana 47907

C. J. Sandberg†

Central Materials Preparation Facility, Purdue University, West Lafayette, Indiana 47907

J. M. Honig

Department of Chemistry, Purdue University, West Lafayette, Indiana 47907

(Received 17 April 1984)

Single crystals of magnetite were grown and annealed under a controlled oxygen atmosphere to produce homogeneous, single phase samples. Heat capacity studies revealed a single, sharp first order heat capacity transition at the Verwey transition $T_V \cong 121$ K, no anomaly at 10 K, no evidence for short range order, and an entropy of transition of $\Delta S_V = R \ln 2$ per mole of Fe₃O₄. A model accounting for this numerical result is discussed.

I. INTRODUCTION

The Verwey electrical transition in Fe₃O₄ has been investigated numerous times, ever since the original report on this phenomenon by Verwey and co-workers.¹ As is by now well established, the electrical resistivity changes by two orders of magnitude over a small temperature interval (< 0.1 – 0.9 K) in the neighborhood of $T_V = 120$ K; the precise value of T_V depends on the oxygen stoichiometry.^{1,2} Despite intense theoretical analysis over a period of several decades the microscopic origin of the electrical transition is not well understood; it seems to be closely linked to charge ordering, but the precise nature of the ionic configuration is still in doubt.³

One of the fundamental techniques for investigating the Verwey anomaly is the measurement of heat capacities. Unfortunately, widely discordant results have been reported in the literature, which makes the resolution of these differences an urgent problem if one is to gain a better understanding of the fundamentals of the transition.

Heat capacity measurements reported in the literature may be divided into three general categories: papers devoted to a study of spin-wave excitations in the cryogenic temperature region,^{4–6} studies which extend over a significant temperature range,^{7–14} and publications devoted primarily to the investigation of the Verwey anomaly.^{15–23}

Two schools of thought have emerged with respect to results obtained both at low temperatures and in the vicinity of the Verwey transition. Tōdō and Chikazumi¹² have encountered a specific heat anomaly centered on 11 K for a single crystal Fe₃O₄ specimen which had been annealed in CO/CO₂ for 10 days at 720°C. However, in other measurements in this temperature range^{9,13,14} on single crystals, no such peak was detected.

Another controversy has arisen concerning the thermal anomaly accompanying the Verwey transition. Westrum

and collaborators,^{10,11,17–19,23} Rigo and co-workers,^{13,22,24} and Kamilov *et al.*²⁰ all have encountered bifurcation effects, i.e., the existence of two closely spaced heat capacity peaks in the temperature range from 100 to 125 K. The precise position of the peaks on the temperature scale, their relative intensities, and their width were found to depend on the nature of the sample (whether single crystal or polycrystalline), the thermal treatment of the specimens, and the extent and nature of the doping levels. In all these cases each peak extended over a temperature interval ranging from 2 to 11 K. These results are considered to provide experimental support for various theories^{25–28} requiring Fe₃O₄ to undergo a series of closely spaced transitions at the Verwey point. By contrast, no bifurcation effects were reported either in the early investigations^{7,8,15} on natural single crystals or in the later measurements^{14,21} on a variety of single crystal or polycrystalline specimens that had been thoroughly annealed. The widths of the peaks in the later studies ranged from 0.3 to 1 K. A final difference of opinion concerns the shift in baseline: Whereas Matsui *et al.*²¹ detected a very marked shift which they interpreted as showing the persistence of short range order up to 400 K, all other investigators report that the heat capacity peak is situated on top of a smoothly continuing background trace.

That the various qualitative differences in results may be associated with sample annealing problems under controlled oxygen atmospheres seems indicated by several preliminary investigations^{14,21} which show that the heat capacity peaks can be shifted or altered qualitatively by changes in sample treatment. In particular, the earlier studies suggest that careful sample handling might narrow the temperature range of the heat capacity anomaly near the Verwey transition temperature. Consequently, the condition of sample growth and preparation will be described in detail, before turning to the discussion of the heat capacity measurements and results.

II. EXPERIMENTAL TECHNIQUE

Samples of magnetite were grown in a skull melter whose operation is discussed elsewhere.²⁹ The skull crucible consists of cylindrical arrangement of closely spaced, individually water-cooled copper tubes on a split base. The crucible was loaded with initially 99.9% pure Fe_2O_3 powder. An rf generator operating at 3 MHz and 50 kW was used as the source of high frequency electromagnetic radiation which was fed to a work coil surrounding the crucible. A graphite ring was used as the susceptor; after coupling to the radiation it heated the contiguous Fe_2O_3 powder sufficiently to initiate coupling of these regions to the radiation source. An avalanching process then ensued such that all of the powder became molten except for a very thin, sintered skull close to the water-cooled container base and crucible fingers. The graphite ring ultimately burned off in the CO_2 atmosphere maintained over the melt.

Single crystals were then produced by a modified Bridgman technique in which the crucible containing the molten Fe_3O_4 was slowly lowered out of the stationary work coil, thereby gradually freezing the melt and forming large single crystals. Pure CO_2 gas was slowly passed through the system during the course of the run to control the composition. The resulting crystals within the boule were slightly cation deficient but remained well within the stability range²⁹ of Fe_3O_4 . The characterization of these crystals is also described in Ref. 29.

In addition, neutron activation studies³⁰ on some samples revealed the following major impurities: 100 ppm Cr, 100 ppm Na, 30 ppm Pb, 30 ppm Ni, and 20 ppm Mn.

After cooling, a small section of a single crystal was reannealed under an appropriate CO/CO_2 atmosphere whose partial oxygen pressure was monitored with a solid state electrochemical cell.³¹ Annealing conditions were determined from the thermogravimetric data of Dieckmann.³² Most samples were annealed at 1400 °C and in the oxygen fugacity range $-5.1 < \log_{10} f_{\text{O}_2} < -4.2$ to yield samples close to the ideal 3/4 iron-to-oxygen stoichiometry ratio.

Two methods of annealing and quenching were employed, one for slow quench in a horizontal furnace, and the second, for fast quench in a vertical furnace. In both cases, the fugacity and temperature were monitored with a solid electrolyte cell containing a type-R thermocouple. Circuitry³³ to calculate and display $\log_{10} f_{\text{O}_2}$ and temperature was used to monitor and adjust annealing conditions.

In the first method, a thin sample (< 0.5 mm) was placed in a Pt boat suspended by Pt wire over an alumina boat. Since the solubility of Fe in Pt is a function of temperature and oxygen fugacity, Pt boats were presaturated by filling with Fe_3O_4 powder and annealing at a particular fugacity and temperature. Subsequently, each boat was used only for annealing samples under its appropriate condition. The sample was quenched by quickly pulling (1–2 sec) the sample from the hot zone (1400 °C) to a region of lower temperature (~ 1000 °C). The sample was then gradually cooled to room temperature over the next 15 min.

In the second method, relatively thick samples (3–5

mm) were placed in a basket of 40-gauge Pt wire; the wire basket was attached to 24-gauge Pt wire at the top of an alumina rod. To quench the sample, current was passed through the Pt wires, thus severing the thin Pt wires and dropping the sample onto fiberfrax matting in a water-cooled end cap.

After quenching, a specimen approximately $5 \times 5 \times 0.7$ mm³ in dimension (40–80 mg) was cut, polished, and mounted in a relaxation calorimeter designed by Griffing and Shivashankar.³⁴ The temperature reservoir consisted of a large copper block which was connected by a heat leak rod to a container filled with cryogenic fluid. The temperature of the reservoir was stabilized by a PAR Model 152 temperature controller that utilized a separate control light emitting diode (LED) temperature sensor. The sample was placed on a sapphire substrate connected by four lead wires to the temperature reservoir. The opposite side of the sapphire contained an evaporated gold heater pattern; an attached, unencapsulated LED temperature sensor³⁵ served as the thermometer. To measure the heat capacity at a particular temperature, constant power was applied to the heater for sufficient time to allow the substrate and sample to reach a steady state temperature ΔT above the baseline temperature T_0 of the reservoir. When the power was turned off, the temperature decayed exponentially to T_0 . The heat capacity is determined from the equations

$$\tau = C_P / \kappa, \quad P = \kappa \Delta T, \quad (1)$$

where C_P is the heat capacity of the sample and substrate, P is the applied power, and κ is the thermal conductance of the wires. The latter is found from the measured temperature difference ΔT and from the electric power input. Griffing and Shivashankar³⁴ estimated that the accuracy of the heat capacity measurement was $\pm 5\%$ below 30 K and $\pm 2\%$ above 30 K. Heat capacity measurements of a large sample of oxygen-free copper agreed with those in the literature to within 1%.³⁶

To investigate first order transitions, the calorimeter was also operated in a transition mode so as to obtain cooling and heating curves in the vicinity of the Verwey temperature. The change in enthalpy ΔH_V of the transition is calculated from the thermodynamic relation

$$\Delta H_V = \int C_P dt = \int [P - \kappa(T - T_0)] dt. \quad (2)$$

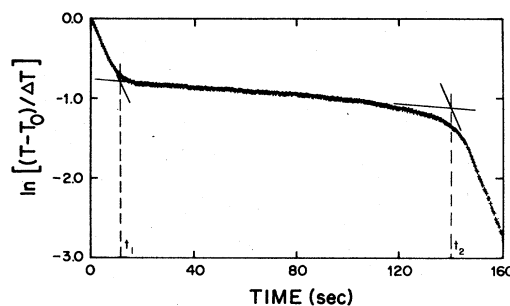


FIG. 1. Plot of $\ln(T - T_0)/\Delta T$ versus time used to determine the starting point t_1 and the ending point t_2 of the first order latent heat region of the cooling curve.

For the heating curve, P is the applied constant power; for the cooling curve, P is zero. The operation of the calorimeter in the transition mode was checked³⁴ by determining the heat of fusion of mercury at 234 K; experimental values obtained in these runs were within 2% of the heats of fusion quoted in the literature.

To pick the starting and ending points of integration for the calculation of the change in enthalpy of the cooling curve, $\ln[(T - T_0)/\Delta T]$ was plotted against the time t . The initial decay, the flat transition region, and the final decay were fitted by least squares to a set of three straight lines. The intersection of these lines gave the starting and ending times. Figure 1 illustrates the technique.

The change in entropy ΔS_V of the transition is given by $\Delta S_V = \Delta H_V / T_V$, where T_V is the average Verwey transition temperature. The estimated accuracy of the change in entropy is $\pm 5\%$. The slight ambiguity in the choice of the starting and ending integration points account for most of the error. The greater error cited here is due to the larger inhomogeneity of Fe_3O_4 relative to the pure mercury sample used by Griffing and Shivashankar³⁴ in their evaluation of the transition mode.

The temperature scale was determined by calibrating the diode against a calibrated Ge resistance thermometer in the temperature range from 4.2 to 100 K and against a Pt thermometer from 75 to 350 K. The accuracy of the temperature measured by the diode varies over the full 4.2–350 K range. The absolute accuracy of the diode temperature is estimated to be better than 0.05 K below 40 K and better than 0.1 K above 40 K. The relative accuracy of the diode temperature is limited to 5 mK by the diode preamplifier unless signal averaging is used.

III. RESULTS AND DISCUSSION

Heat capacity curves for two nearly stoichiometric Fe_3O_4 specimens in the range 5–340 K are shown in Figs. 2(a) and 2(b), respectively; these are quite typical of the remaining measurements on three other samples. The base curves all coincide within experimental error. The various curves differ only in the shape of the heat capacity peak. In all samples, very small premonitory and post-monitory effects were encountered in a ± 3 -K interval about the Verwey transition at 121 K. As explained below, no evidence was found for short range order outside this interval. The entropy change in this range is of the order of $\Delta S = 0.25$ J/mol K of Fe_3O_4 , less than 5% of the entropy change corresponding to the latent heat. By contrast to these very shallow shoulders, the principal heat capacity anomaly resides in a very narrow peak corresponding to the latent heat of the Verwey transition. This peak tends to be vestigial [as in Figs. 2(a) and 3(a)] because of the problem of spacing successive measurements over sufficiently small temperature intervals for proper scanning of the peak. Our heat capacity measurements agree with the results of most other experiments, except in the region near the Verwey transition, to better than $\pm 5\%$. The crucial differences near the Verwey transition can be attributed to sample preparation and are discussed below.

To analyze the first order transition, one must resort to

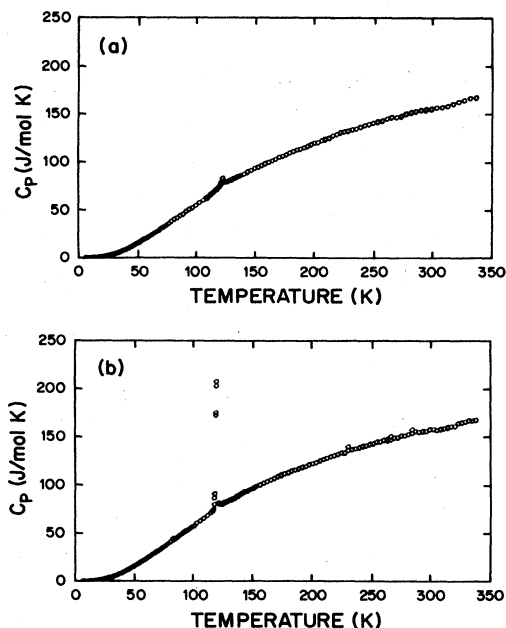


FIG. 2. (a) Specific heat of stoichiometric Fe_3O_4 from 5 to 350 K. (b) Specific heat of a stoichiometric sample with a broader transition. The small dip in the heat capacity at ~ 310 K is due to a slight error in the thermometer fit in that region.

the use of cooling or heating curves as detailed below. A more detailed view of the anomalous region is provided in Figs. 3(a) and 3(b); it is seen that the temperature span at the base of the heat capacity spike is in the neighborhood of ± 2 –3 K, which again is typical of all the studies in this series.

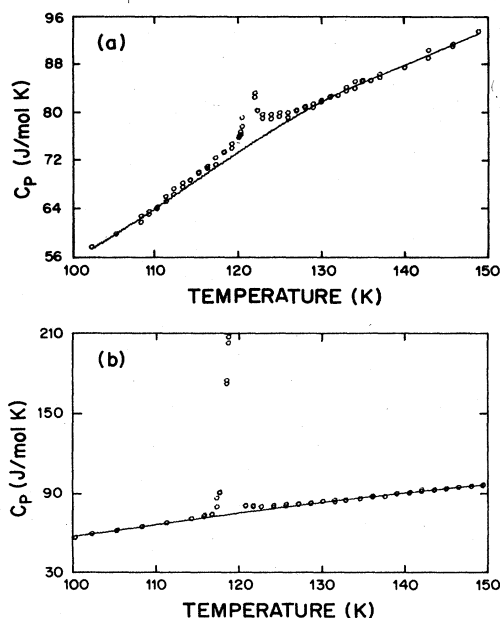


FIG. 3. (a) Specific heat showing the Verwey transition in detail. Note the vestigial peak in this sample. (b) Specific heat anomaly at the Verwey transition of a sample with a broader transition.

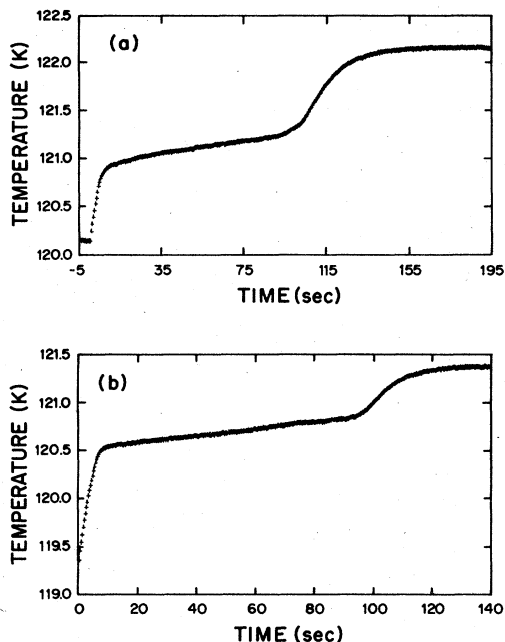


FIG. 4. Heating curves showing the first order transition of two stoichiometric samples, (a) and (b).

More insight on the transition is gained by examining the heating and cooling curves shown in Figs. 4(a) and 4(b) and 5(a) and 5(b), respectively. These clearly show the interruption of the exponential decay curves typical of first order transitions. One should note the temperature scale on the ordinate: The transformation takes place over an interval of not more than 0.4 K; also, the hys-

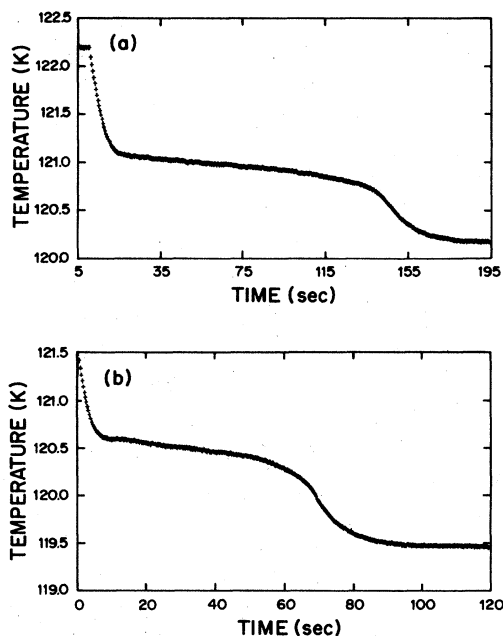


FIG. 5. Cooling curves showing the first-order transition of two stoichiometric samples, (a) and (b).

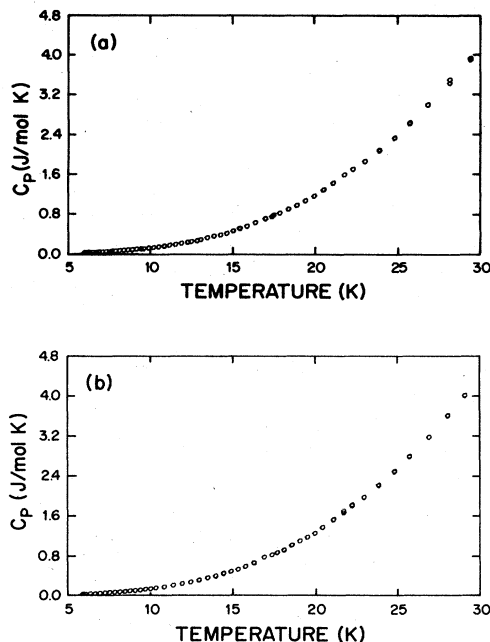


FIG. 6. Specific heat of two samples (a) and (b) in the region 0 to 30 K. There is no indication of any specific heat anomaly at 10 K.

teresis for the heating as opposed to the cooling cycle is in the neighborhood of 0.3 K. The above values are quite typical for the entire series. Finally, Figs. 6(a) and 6(b) show an enlargement of the low temperature range between 0 and 30 K; no specific heat anomaly is detectable in this range. This is also the case for all of the remaining measurements listed in Table I.

A summary of all the experimental findings is provided in Table I. The following general conclusions may be drawn:

(1) For all the specimens investigated in this series a heat capacity anomaly is encountered in the range 120–122 K. From independent measurements of resistivity and from thermomagnetic analysis of specimens prepared under the same experimental conditions,³⁷ it is evident that the heat capacity peak is associated with the Verwey transition.

The results cited in Table I should be compared with those shown in Table II as assembled from the literature. The Verwey temperatures T_V reported for carefully annealed single crystals of reasonable purity fall in the range 121.7 to 123.6 K (Refs. 14 and 21) which is somewhat higher than the values cited in Table I; however, because of the general absence of published information on temperature calibrations, it can be argued that the results of Refs. 14 and 21 and those reported here are comparable. The marked decrease in T_V with increasing dopant or vacancy concentration should also be noted: this is a universal phenomenon, showing the sensitivity of the phase transition temperature to the Fe^{2+} -to- Fe^{3+} ratio in the host lattice.

(2) In conformity with the data reported in Refs. 7, 8, 14, 15, and 21, we observed only a single heat capacity peak, a fact which seems to render dubious the applicabil-

TABLE I. Experimental results on the Verwey transition. Values listed are the entropy of transition (\pm variance), average transition temperature, upper limit on the width of the transition, hysteresis between heating and cooling transitions, and the total temperature difference the sample traversed during the measurement.

Sample	S (J/mol K) ^a	T_V (K)	Width (K)	Hysteresis (K)	ΔT (K)
1	5.88(\pm 0.05)	121.3	0.37	0.5	1.83
1	5.98(\pm 0.05)	120.8	0.49	0.5	2.22
2	5.98(\pm 0.14)	120.7	0.4	0.26	2.00
2	5.96(\pm 0.13)	120.5	0.5	0.26	2.00
2	5.84(\pm 0.07)	120.7	0.35	0.25	1.00
2	5.83(\pm 0.01)	120.5	0.35	0.25	1.00
3	6.08(\pm 0.03)	121.1	0.5	0.18	2.00
3	6.00(\pm 0.07)	120.9	0.5	0.18	2.00
3	5.63(\pm 0.09)	120.9	0.5	0.18	1.50

^aStatistical error is shown. The experimental error is estimated to be below 5%. The contribution $\Delta S \cong 0.25$ J/mol K of Fe_3O_4 due to the premonitory and postmonitory effects is not included.

TABLE II. Summary of the literature data pertaining to the Verwey transition and the entropy of transition. DTA denotes differential thermal analysis.

Reference	T_V (K) Peak of C_p anomaly	ΔS_V (J/mol Fe_3O_4 K)	Sample treatment ^a
7	~115.0	5.44	Natural crystal
8	114.2	4.39	Natural crystal
15 (DTA)	115.0		
9	113.0, 119.0	5.65	Natural crystal
17	117.0, 123.0	7.53	0.2 at. % Mn
18	113.3, 118.9	5.86	Ceramic Fe_3O_4
10,19	(119), 117.3	5.02	Natural crystal containing Zn
	110.6, 119.1	4.60	0.5 at. % Zn
	80.0	3.64	0.66 at. % Zn
	114.7	5.44	0.5 at. % Cd
	105.7	4.11	1.0 at. % Cd
11	117.0, 123.0	4.93	0.8 at. % Mn
21	122.7	5.4+4.2	Single crystal, well annealed
22	114.0, 122.0	2.88	Fe_3O_4 powder
	119.0	2.88	$\text{Fe}_3\text{O}_{4-x}\text{F}_x$, $x=0.1$
	120	2.88	$\text{Fe}_3\text{O}_{4-x}\text{F}_x$, $x=0.25$
23	103.0, 107.0	4.77 to 5.40	0.2 at. % Cd
	107.0, 121.0	4.94	1 at. % Zn
24	114.0, 122.0	5.86	Fe_3O_4 powder
14	123.6	6.24	Single crystal, $c < 5 \times 10^{-6}$
	116.6	5.44	Single crystal, $c = 1.5 \times 10^{-2}$
	122.8	4.77	Powdered crystal, $c = 10^{-5}$
	122.8	5.40	Powdered crystal, $c = 10^{-5}$
	121.6	4.73	Polycrystalline, $c = 4 \times 10^{-4}$
	118.4	4.14	Polycrystalline, $c = 2 \times 10^{-3}$
13	113.5, 125.0	7.95	Single crystal

^a c represents the fractional vacancy concentration.

ity of models for multiple phase transformations.

(3) The transition occurs over an interval of less than 0.5 K. These results agree very well with those reported for carefully annealed specimens in one earlier experiment by Chikazumi and co-workers²¹ and in subsequent work by Gmelin *et al.*,¹⁴ published just prior to completion of our own experiments.

(4) The transition is of first order; this is evident not only from the sharp heat capacity peaks but also from the heating and cooling curves which are of the standard form expected for first order phase changes accompanied by latent heat effects. As far as could be ascertained, this is the first published report of such curves for Fe₃O₄.

There are slight hysteresis effects as revealed in the temperature aspects of the cooling versus the heating curves. The hysteresis encountered here is no greater than 0.3 K, as compared to 2–3 K hysteresis effects reported by Gmelin *et al.*¹⁴ The reasons for this discrepancy are not presently understood.

(5) There is no offset in the baseline above as compared to below the transition temperature; thus, claims²¹ concerning the occurrence of short range order which disappears in a temperature range of 50 to 275 K above the transformation could not be substantiated.

(6) Lastly, the entropies of transition could be directly determined from the various cooling or heating curves. As shown in Table I, these average values range from 5.6 to 6.0 J/mol K Fe₃O₄. Entropy values for individual curves ranged from 5.57 to 6.22 J/mol K Fe₃O₄. The errors given for the entropy are statistical errors; experimental errors could be as much as 5%. The entropy contribution from the small premonitory and postmonitory regions near the transition was estimated by spline fitting³⁸ the heat capacity data in the temperature regions 20–110 K and 130–200 K; this spline was subtracted from the data and the entropy was calculated in the region from 110 to 130 K. In all cases, the entropy contribution from this region was less than 5%.

The lower limit for the entropy was approached under conditions where the heat exchange rate is minimized, i.e., when the temperature rise through the heat pulse is less than 1 K. The values of Table I approach the entropy change of $\Delta S_V = R \ln 2 = 5.765$ J/mol K of Fe₃O₄. This result may be compared to the ΔS_V values listed in Table II, which range from 2.88 to 7.95 J/mol K; for the best crystals listed in that tabulation, the ΔS_V values are 5.4, 6.24, and 5.44 J/mol K.^{14,21} It should be noted that many values compiled in Table II were calculated from areas under the heat capacity peaks; this procedure is subject to considerable error in situations where such peaks are narrow and tall. Nonetheless, it is evident from Table II that either departures from the strict 4/3 oxygen-to-cation ratio or the doping of the host lattice with foreign substituents drastically reduces the ΔS_V values.

We lack a unique explanation for our observed values of $\Delta S_V = R \ln 2$. However, it is clear that the commonly cited theoretical estimate of $\Delta S_V = 2R \ln 2$ /mol Fe₃O₄ is based on a simulation in which the Verwey transition is modeled by the formation of a binary random mixture from two pure phases, *A* and *B*.

One way of rationalizing our experimental values for

ΔS_V is to take account of the structural features of the Fe²⁺, Fe³⁺ distribution below the Verwey transition. As shown by Kita *et al.*,³⁹ one structural arrangement of $A \equiv \text{Fe}^{2+}$ and $B \equiv \text{Fe}^{3+}$ sites for $T < T_V$ which satisfies the neutron and x-ray diffraction results, as well as the NMR studies, is a configuration of chains of the type . . . , *AA, BB, AA, BB, AA, BB, . . .* along one of the [110] directions in the *B* planes of the cations. The interchain distance is almost 1.8 times the value of the intrachain distances and will be ignored. This type of ordering may be modeled by use of order-disorder theory as developed by Hijmans and de Boer;⁴⁰ for reviews, see Refs. 41 and 42. In general terms, the entropy for a lattice represented as a collection of "bonds" and "points" is given by

$$\frac{S}{k_B L} = -\frac{Z}{2}(\beta_0 \ln \beta_0 + 2\beta_1 \ln \beta_1 + \beta_2 \ln \beta_2) - (1-Z)(\alpha_0 \ln \alpha_0 + \alpha_1 \ln \alpha_1). \quad (3)$$

In addition, the consistency and normalization relations

$$\alpha_0 = \beta_0 + \beta_1, \quad \alpha_1 = \beta_1 + \beta_2, \quad \alpha_0 + \alpha_1 = 1 \quad (4)$$

are relevant. In the above, k_B is Boltzmann's constant; L is the number of octahedral sites in the spinel lattice occupied by cations ($L = 2N_A$, where N_A is Avogadro's number for one mole of Fe₃O₄); Z is the coordination number; β_0 , $2\beta_1$, and β_2 are the probabilities of encountering the *AA*, *AB* or *BA*, and *BB* bond configurations, respectively, and α_0 and α_1 are the probabilities of encountering the *A* and *B* site configurations, respectively.

In the situation under discussion, the ordered configuration of Kita *et al.*³⁹ is represented by the numerical assignments $Z = 1$, $\alpha_0 = \alpha_1 = \frac{1}{2}$, $\beta_1 = 0$, $\beta_0 = \beta_2 = \frac{1}{2}$, which immediately leads to the value $S_0 = R \ln 2$.

In the disordered phase one considers the lattice as a collection of sites for which

$$\frac{S}{k_B L} = -(\alpha_0 \ln \alpha_0 + \alpha_1 \ln \alpha_1). \quad (5)$$

For $L = 2N_A$ and $\alpha_0 = \alpha_1 = \frac{1}{2}$, this leads to the value $S_d = 2R \ln 2$. Thus $\Delta S_V = S_d - S_0 = R \ln 2$ /mol Fe₃O₄, in conformity with observation.

Scant physical significance should be paid to the details of the above treatment. The exposition is meant to render plausible the interpretation of $\Delta S_V = R \ln 2$ as being consistent with (among other possibilities) a segregation of cations into Fe²⁺-Fe²⁺ and Fe³⁺-Fe³⁺ pairs along specific directions on *B* planes in magnetite. Many other types of pairings have been proposed, though the configurations of Mizoguchi⁴³ and Iida² have been criticized³ as being incompatible with structural information.

It should be recognized that $\Delta S_V = R \ln 2$ should represent an upper limit to the entropy change as specified by the above crude model. Any deviations from strict stoichiometry, as well as interactions among electrons which lead to a less than complete random distribution of electrons in the disordered phase, would diminish ΔS_V . The present theory is too crude to provide a reliable estimate of these factors; a more sophisticated theory would have to be invoked to settle these delicate matters. Addi-

tionally, it would seem premature to make more detailed calculations until the nature of the ordered state in magnetite is properly settled.

IV. CONCLUSIONS

It has been established in this work that through careful preparative methods stoichiometric Fe_3O_4 samples of sufficient homogeneity can be prepared such that a single first order phase transition is encountered near 121 K. The latter is associated with an entropy change of approximately $R \ln 2$ per mole of Fe_3O_4 . No evidence is found for the existence of other thermal anomalies, bifurcation effects, or the existence of short range order above the Verwey transition temperature. Deviations from the exact

Fe_3O_4 composition result in a lowering of the transition temperature and of the concomitant entropy change. A model invoking the alternation of Fe^{2+} - Fe^{2+} and Fe^{3+} - Fe^{3+} pairs along [110] directions on B planes provides a rationalization of the observed entropy changes.

ACKNOWLEDGMENTS

The authors are greatly indebted to Dr. Harold Harrison for valuable advice and assistance in the growth and preparation of crystals for this research project. This research was supported by Grant No. DMR-81-03041-A02 of the National Science Foundation. The skull melter unit was acquired on NSF Grant No. DMR-79-11137.

*Present address: Kodak Research Laboratories, Kodak Park, Rochester, NY 14650.

†Present address: Rockwell International Science Center, Thousand Oaks, CA 91360.

¹E. J. W. Verwey and P. W. Haayman, *Physica (Utrecht)* **8**, 979 (1941).

²S. Iida, *Philos. Mag. B* **24**, 349 (1980).

³M. Iizumi, T. F. Koetzle, G. Shirane, S. Chikazumi, M. Matsui, and S. Tōdō, *Acta Crystallogr. Sect. B* **38**, 2121 (1982).

⁴J. S. Kouvel, *Phys. Rev.* **102**, 1489 (1956).

⁵R. K. Kenan, M. L. Glasser, and F. J. Milford, *Phys. Rev.* **132**, 47 (1963).

⁶M. Dixon, F. E. Hoare, and T. M. Holden, *Phys. Lett.* **14**, 184 (1965).

⁷G. S. Parks and K. K. Kelley, *J. Phys. Chem.* **30**, 47 (1926).

⁸Russell W. Millar, *J. Am. Chem. Soc.* **51**, 215 (1928).

⁹Edgar F. Westrum, Jr. and Fredrik Grønvold, *J. Chem. Thermodyn.* **1**, 543 (1969).

¹⁰James J. Bartel and Edgar F. Westrum Jr., *J. Chem. Thermodyn.* **8**, 583 (1976).

¹¹James J. Bartel, Edgar F. Westrum Jr., and John L. Haas Jr., *J. Chem. Thermodyn.* **8**, 575 (1976).

¹²Sakae Tōdō and Sōshin Chikazumi, *J. Phys. Soc. Jpn.* **43**, 1091 (1977).

¹³M. O. Rigo, J. F. Mareche, and V. A. M. Brabers, *Philos. Mag. B* **48**, 421 (1983).

¹⁴E. Gmelin, N. Lenge, and H. Kronmüller, *Phys. Status Solidi A* **79**, 465 (1983).

¹⁵T. Okamura, *Sci. Rep. Tohoku Imp. Univ. Ser. 1* **21**, 231 (1932).

¹⁶T. Okamura and Y. Torizuka, *Sci. Rep. Res. Inst. Tohoku Imp. Univ. Ser. A* **2**, 352 (1950).

¹⁷B. J. Evans and E. F. Westrum, Jr., *Phys. Rev. B* **5**, 3791 (1972).

¹⁸J. J. Bartel and E. F. Westrum, in *Magnetism and Magnetic Materials—1972 (Denver)*, proceedings of the 18th Annual Conference on Magnetism and Magnetic Materials, edited by C. D. Graham and J. J. Rhyne (AIP, New York, 1972), p. 1393.

¹⁹J. J. Bartel and E. F. Westrum, in *Magnetism and Magnetic Materials—1974 (San Francisco)*, proceedings of the 20th An-

nual Conference on Magnetism and Magnetic Materials, edited by C. D. Graham, G. H. Lander, and J. J. Rhyne (AIP, New York, 1975), p. 86.

²⁰I. K. Kamilov, G. G. Musaev, and G. M. Shakhshae, *Dokl. Akad. Nauk SSSR* **220**, 1057 (1975). [*Sov. Phys. Dokl.* **20**, 121 (1975)].

²¹Masaaki Matsui, Sakae Tōdō, and Sōshin Chikazumi, *J. Phys. Soc. Jpn.* **42**, 1517 (1977).

²²M. O. Rigo, J. Kleinclauss, and A. J. Pointon, *Solid State Commun.* **28**, 1013 (1978).

²³G. B. Falk, L.-S. Pan, B. J. Evans, and E. F. Westrum Jr., *J. Chem. Thermodyn.* **11**, 367 (1979).

²⁴M. O. Rigo and J. Kleinclauss, *Philos. Mag. B* **42**, 393 (1980).

²⁵J. R. Cullen and E. Callen, *Phys. Rev. Lett.* **26**, 236 (1971).

²⁶J. R. Cullen and E. Callen, *Phys. Rev. B* **7**, 397 (1971).

²⁷D. Ihle and B. Lorenz, *Phys. Status Solidi B* **58**, 79 (1973).

²⁸D. Ihle and B. Lorenz, *Philos. Mag. B* **42**, 337 (1980).

²⁹Harold R. Harrison and Ricardo Aragón, *Mater. Res. Bull.* **13**, 1097 (1978).

³⁰We wish to thank M. Yethiraj of the Missouri University Research Reactor for carrying out the analysis.

³¹Motoaki Sato, in *Research Techniques for High Pressure and High Temperature*, edited by Gene C. Ulmer (Springer, New York, 1971), pp. 43–99.

³²R. Dieckmann, *Ber. Bunsenges. Phys. Chem.* **86**, 112 (1982).

³³John P. Shepherd and Charles J. Sandberg, *Rev. Sci. Instrum.* (to be published).

³⁴B. F. Griffing and S. A. Shivashankar, *Rev. Sci. Instrum.* **51**, 1030 (1980).

³⁵B. F. Griffing and S. A. Shivashankar, *Rev. Sci. Instrum.* **48**, 1255 (1977).

³⁶Bruce Griffing (personal communication).

³⁷D. Buttrey, M. Pai, and R. Aragón (unpublished).

³⁸P. Dierceux, *J. Comp. Appl. Math.* **1**, 165 (1975).

³⁹Eiji Kita, Yuko Tokuyama, Akira Tasaki, and Kiiti Siratori, *J. Magn. Magn. Mat.* **31–34**, 787 (1983).

⁴⁰J. Hijmans and J. de Boer, *Physica (Utrecht)* **21**, 471 (1955); **21**, 485 (1955); **21**, 499 (1955).

⁴¹C. Domb, *Adv. Phys.* **9**, 149 (1960).

⁴²J. M. Honig, *J. Chem. Ed.* **38**, 538 (1961).

⁴³M. Mizoguchi, *J. Phys. Soc. Jpn.* **44**, 1512 (1978).